nature portfolio

https://doi.org/10.1038/s41586-021-04147-1

Supplementary information

Bizarre tail weaponry in a transitional ankylosaur from subantarctic Chile

In the format provided by the authors and unedited

Supplementary Information

Bizarre tail weaponry in a transitional ankylosaur from subantarctic Chile

Sergio Soto-Acuña, Alexander O. Vargas, Jonatan Kaluza, Marcelo A. Leppe, Joao F. Botelho, José Palma-Liberona, Carolina Simon-Gutstein, Roy A. Fernández, Héctor Ortiz, Verónica Milla, Bárbara Aravena, Leslie M.E. Manríquez, Jhonatan Alarcón-Muñoz, Juan Pablo Pino, Christine Trevisan, Héctor Mansilla, Luis Felipe Hinojosa, Vicente Muñoz-Walther, and David Rubilar-Rogers

†email: sesotacu@ug.uchile.cl, alexvargas@uchile.cl

This PDF file includes:

Supplementary text:

1. Taphonomical aspects of the holotype

The holotype of *Stegouros* was found semi-articulated, partially exposed in a slope within a coarse to medium grain sandstone level, featuring some centimetric mudstone intercalations (Supplementary Fig. 1). The whole skeleton lay within a vertical range of approximately 40 cm (Supplementary Fig. 2a, b). These layers are interpreted locally as the bar of a river in a meandering fluvial system (Supplementary Fig. 3). The posterior half of the skeleton, including most of the pelvis, hindlimbs, and tail was articulated. In contrast, the anterior half of the skeleton was mostly disarticulated but closely associated in an area of approximately 2 m^2. The posterior half of the skeleton was also the portion lying deepest with respect to the sandy (bottom) to muddy (top) layers of sediment (Supplementary Data Fig. 2b). The skeleton was not overturned, with its dorsal aspect facing upward. The proximal portion of the tail was bent into a "zig-zag" below the pelvis, with the distal tail closer to the pelvic girdle than would be expected in its natural extended position. Within the articulated half of the skeleton, portions of some elements are absent, such as part of the right diaphysis of the tibia and fibula. This is likely due to diagenetic alteration marked by the presence of joints (diaclases) which were mapped in relation to bone positions and orientation (Supplementary Fig. 2a). One joint plane also coincides with the breakage and unnatural position of the proximal tail, and the missing posterior half of the 18th caudal vertebra, distal to which all vertebrae within the caudal weapon are missing (supplementary video 1). This brings up the possibility that the joint may have led to conditions within the tail weapon that were unfavourable for preservation of these vertebrae. A directional analysis (rose diagram) was performed using PAST 4.0 [42] (Supplementary Fig. 2c). Due to extreme field conditions and challenging weather, the direction of some dorsal ribs, some cervical ribs, left sternal plate, right radius, ulna, and articulated manus were not measured in the field. Their positions shown in the quarry map are according to observations made during the preparation process. A list of elements was made, considering those recovered at the quarry and throughout the preparation of the five jackets processed in the laboratory (Supplementary Table I). The presence/absence of elements was then compared to attributed susceptibility to transportation of the Voorhies groups [43], taking into consideration the revisions undertaken by several authors [44-47]. The recovered disarticulated elements were consistent with the skeletal composition and proportions expected for a single individual, since no duplicated elements were found, and every element had a consistent size and proportion (Supplementary Table I). Moreover, the articulated portion has a similar surface texture to the associated anterior portion of the specimen. The directional analysis showed a preferred trend to the NW-SE (Supplementary Fig.1c; $p<0.05$)- Accordingly, the palaeocurrent direction measured in the trough cross-bedding structure of the sandstone bed at the bottom of the deposition site was of NW direction (290º). The top layer of the depositional site had no visible sedimentary structures that denote any movement by currents, being thinner in granulometry (Supplementary Fig.3c, d) and therefore interpreted as a calmer deposition environment at the final part

of this portion of the sequence. On the other hand, no alteration of the bone was observed regarding abrasion or wear pattern (which could be obscured by diagenetic processes) and the analysis of presence/absence of elements based on expected skeletal completeness is unrelated to water transportation for most of the transportability classifications. For example, most of the phalanges are present, as well as most vertebrae, ribs, sacrum, ilia (groups I and II, sensu [43,46]). Meanwhile, the elements that are missing include scapulae and vertebrae, including the more distal caudal vertebrae within the caudal weapon (group I or II of [43,46]; group I of [47]), some of the cranial bones (group III for all authors, including[44]) and most of the left dentary (Group II or III [43,46]; Group I of [47]).

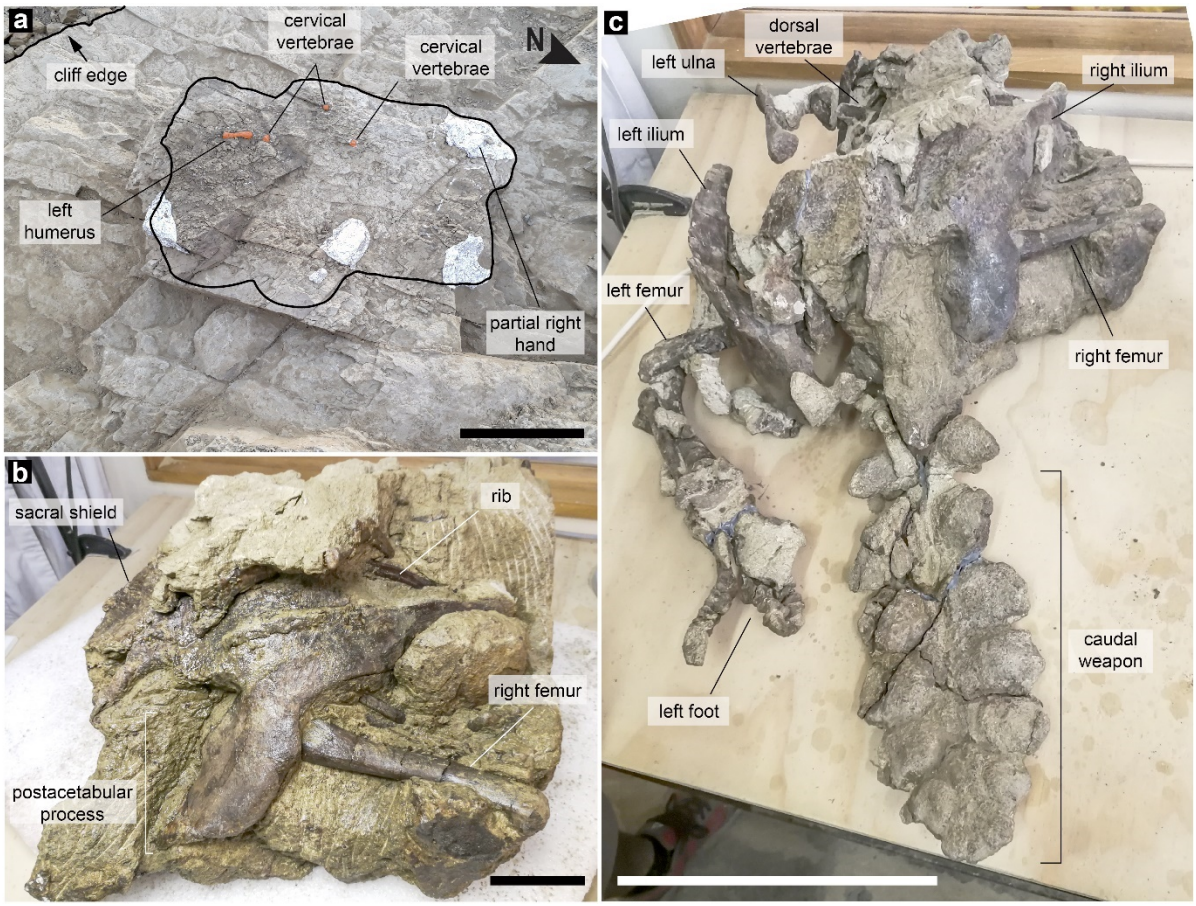

Supplementary Fig. 1 Excavation and preparation of the holotype of *Stegouros elengassen*. a, photo of the excavation site indicating the few elements exposed on the surface. Outline indicates the recovered blocks. **b,** photo of the pelvis and right femur still embedded in a rocky matrix, in the process of mechanical removal. **c,** photo of the articulated portion of the skeleton in preparation. The right posterior limb was preserved in a concretion separated by a joint and was previously removed in the field. Scale bars for a and c = 50 cm, b = 10 cm.

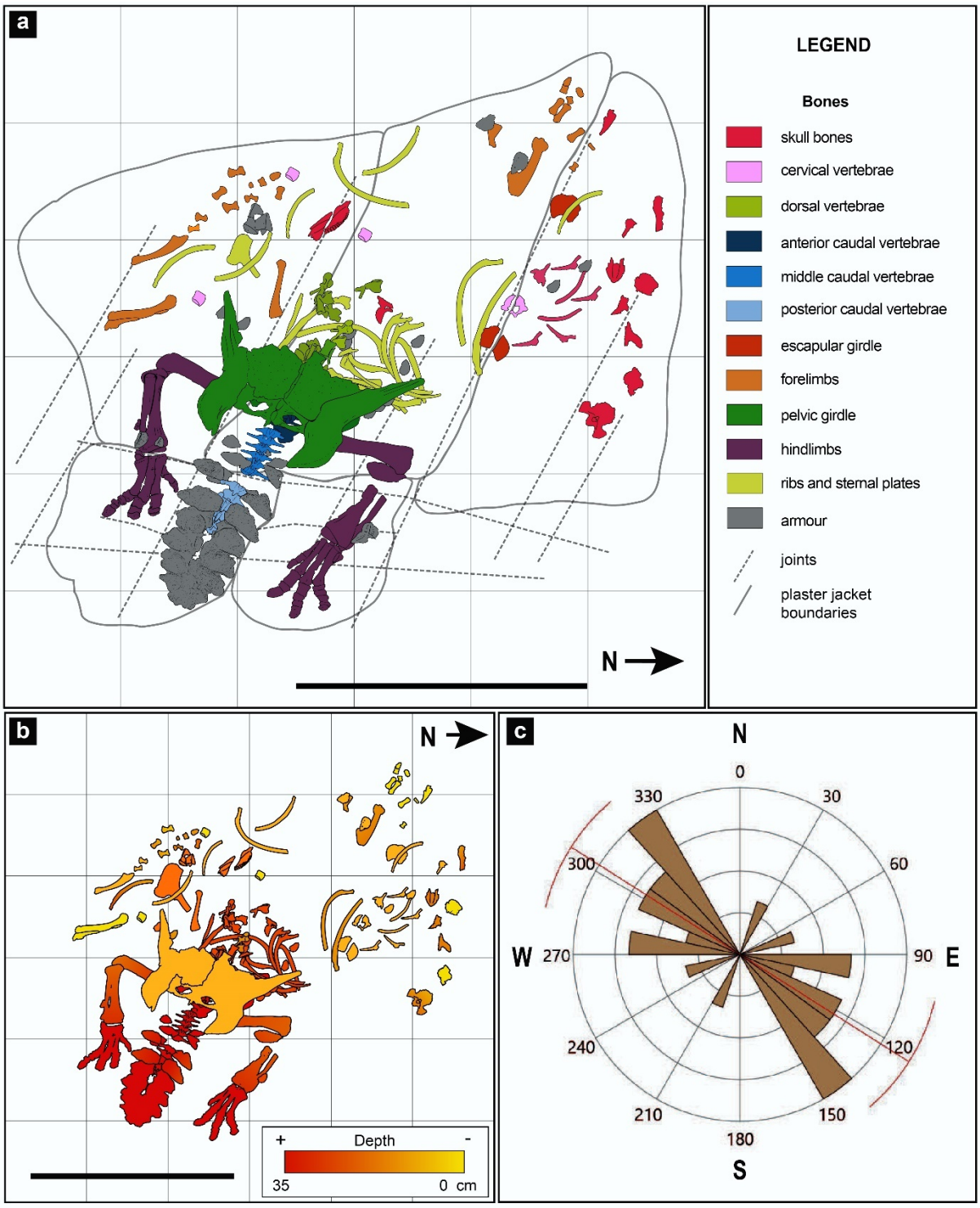

Supplementary Fig. 2 Taphonomic information on the excavation of the holotype of *Stegouros elengassen*. a, Quarry map showing the distribution of bones, reconstructed from field data and preparation of the jackets. **b,** Quarry map showing the depth of the skeletal elements in the sedimentary layers. **c,** Rose diagram of the long bones and axial skeleton of the posterior portion of the holotype of *Stegouros elengassen.* The red line shows the average trend in degrees with respect to the North (0). Scale 50 cm (Grid 20 cm)

Supplementary Table I: List of preserved bones of *Stegouros elengassen* gen. et sp. nov

Skull bones	Forelimb bones	Left hindlimb bones	Right hindlimb bones	Axial postcranial bones	Pelvic girdle bones
Rostral premaxilla	Left humerus	Left femur	Right femur	Axis	Left ilium
Left maxilla	Left radius	Left tibia	Right tibia	4 Postaxial cervical vertebrae	Left ischium
Right maxilla	Left ulna	Left metatarsal I	Right metatarsal I	10 Dorsal Vertebrae	Right ilium
Left supraorbital?	Left metacarpal I	Left phalanx I-1	Right phalanx I-1	2 Dorsosacral vertebrae	Right ischium
Right prefrontal?	Left metacarpal II	Left phalanx I-2	Right phalanx I-2	4 sacral vertebrae	**Scapular girdle bones**
Occipital complex	Left metacarpal III	Left metatarsal II	Right metatarsal II	12 proximal caudal vertebrae	Left coracoid
Left prootic	Left metacarpal IV	Left phalanx II-1	Right phalanx II-1	5 distal caudal vertebrae	Right coracoid
Basisphenoid	Left metacarpal V	Left phalanx II-2	Right phalanx II-2	Left sternal plate	**Osteoderms**
Predentary	Right metacarpal I	Left phalanx II-3	Right phalanx II-3	Right sternal plate	Sacral shield
8 isolated teeth	Right phalanx I-1	Left metatarsal III	Right metatarsal III		7 limb osteoderms
Middle fragment of left dentary	Right phalanx I-2	Left phalanx III-1	Right phalanx III-1		12 isolated osteoderms
Right dentary	Right metacarpal II	Left phalanx III-2	Right phalanx III-2		7 free caudal osteoderms
	Right phalanx II-1	Left phalanx III-3	Right phalanx III-3		Caudal weapon
	Right phalanx II-2	Left phalanx III-4	Right phalanx III-4		
		Left metatarsal IV	Right metatarsal IV		

		Left phalanx IV-1	Right phalanx IV-1		
		Left phalanx IV-2	Right phalanx IV-2		
		Left phalanx IV-3	Right phalanx IV-3		
		Left phalanx IV-4	Right phalanx IV-4		
		Left phalanx IV-5	Right phalanx IV-5		
			Right metatarsal V		

It is possible that missing skull elements were removed by recent weathering of the site, considering that skull elements were found in disarticulation, and lied within the first 5 to 10 cm of depth in the sediment. Nevertheless, no recovered skull bone was extensively exposed at the moment of the excavation. Since there is an observed directional trend, but not an expected pattern of bone removal, it is possible that hydrodynamic transportation is one of the factors of bone dispersion, but not entirely responsible for the resulting pattern. In turn, combined action of breakage and disarticulation through biotic activity and later redirection through a weak hydraulic transport could explain the scattering of these bones through breakage and forced disarticulation of the skull and neck (although there are no evident scavenging marks) and some degree of trampling or scavenging related to delayed burial of the anterior portion of the skeleton. Given that this skeleton differs from the most common upside-down position for floating ankylosaur carcasses (as analysed by [48]), if there was any transportation of the entire carcass, it would have been for a rather short distance, without time for bloating. A plausible explanation to the whole ensemble would be rapid burial of the posterior portion, or as a dead carcass floating down the river, deposited at the river bar and rapidly buried [49]. Meanwhile, the anterior portion could be slightly dispersed by a low energy water current as scavenging disarticulated and dispersed the remaining exposed bones, for a longer time span during which the anterior portion remained exposed. The possibility of a floating carcass has the significant directional trend to its favour (both articulated and associated portions of the skeleton) but would not suppose a very long transportation stage from its original death place, given articulation[46] and no evidence for bloating (according to[48]). If the unnatural breakage of the tail and its missing distal caudal vertebrae are diagenetic and related to the associated joints, a quicksand death trap scenario remains plausible. This can be argued from the lower depth of the skeleton based on its exquisite preservation of almost perfectly articulated bones, the skull and vertebral column twisted to the side[49], and extended legs which are unusual for a floating

carcass. In any scenario, there is no evidence of an accumulation site, with a single specimen present, which could be autochthonous to parautochthonous, having been deposited near its original death time and place, at least in the same river system and in a somewhat humid environment, given that there are no signs of extensive desiccation or tendon contraction in the entire skeleton.

2. Geological and Paleoenvironmental context

2.1. Geographical and Stratigraphic Provenance

The holotype of *Stegouros elengassen* gen. et sp. nov. CPAP-3165 was discovered in the Río de las Chinas Valley (50° 42' 42.72'' S /72° 32' 29, 08'' W) in beds from the lower part of the Dorotea Formation located in the Estancia Cerro Guido, northwest to the Torres del Paine National Park, Ultima Esperanza Province, Magallanes Region, Chile (Supplementary Fig. 3a, b).

The Late Cretaceous strata of Ultima Esperanza Province were deposited over the Magallanes/Austral foreland basin. This basin was formed during the Andean compressional orogenesis[50,51], associated with the initial break-up of Gondwana and the opening of the Atlantic Ocean [52,53]. The Upper Cretaceous-Paleogene succession in the Rio de las Chinas Valley includes the following formations in ascending order (Supplementary Fig. 3a): Tres Pasos Formation assigned to Campanian – lower Maastrichtian [54-57], Dorotea Formation, upper Campanian-Danian[10,57-59] and Man Aike Formation assigned to middle Eocene [10,11,57,59-64].

The Dorotea Formation[65] is characterized as a coastal environment, shoreface and delta influenced by tides [11,55,63,66,67]. It is constituted by 1250 - 900 m of thick, predominantly sandstones of different granulometries, frequent conglomerate lenses, and thin beds of calcareous sandy concretions and mudstones (Supplementary Fig. 3c). In addition, this unit includes abundant fossils of marine invertebrates (bivalves, gastropods, among others) and vertebrates, among which are the remains of sharks, anurans, mammals, plesiosaurs, mosasaurs, turtles and dinosaurs including birds[68-76], as well as mudstones with micro and macroflora (pollen, plant remains and wood[11,63,65,77-79].

The skeleton of *Stegouros elengassen* was collected from the Sauropodo locality (SP-17 stratigraphic column, Supplementary Fig. 3c) found in the middle part of the valley, about a distance of 250 m from where the holotypes of the mammals *Magallanodon baikaskenke* and *Orretherium tzen* were discovered[74,76]. The fossil-bearing level corresponds to medium- to coarse-grained sandstones with trough cross-bedding of 1 m thickness (Supplementary Fig. 3d). The depositional environment of the

sandstone bed with *Stegouros* is interpreted as a channel-bar deposit, associated to meandering fluvial system. U-Pb maximum depositional age above and below the *Stegouros* horizons provides values between 71.7 ± 1.2 Ma and 74.9 ± 2.1 Ma[10] supporting an upper Campanian - lower Maastrichtian age for the fossil-bearing levels (Supplementary Fig. 3c).

2.2. The Sauropodo Locality Flora

The palaeoflora of the Sauropodo locality was found in mudstones deposited in floodplain facies of a meandering fluvial system, a few meters above the sandstone sequence that bears *Stegouros* remains[11]. The fossil flora consists mainly of palynomorphs, and macrofossil remains of compressed stems, tree branches, sterile and fertile pinnae of ferns, and leaves, predominantly ferns and angiosperms (Supplementary Fig. 3e-h). The pteridophytic fossils belong to Equisetaceae, Gleicheniaceae, Dicksoniaceae and Cyatheaceae. Gymnosperms were only represented in the microflora, with pollen grains of Podocarpaceae and Araucariaceae. Angiosperm diversity is dominated by pollen grains assigned to Proteaceae, Arecaceae and Liliaceae, while leaf imprints show affinities with Lauraceae, Rosaceae and monocot imprints tentatively classified as Typhaceae. The dicot leaves are notoriously mesophyll-sized (*sensu*[80]), with remarkable preservation of details such as 5th order venation and areolation. Monocot leaf fragments are large, with a broad midrib and parallel venation (Fig. 3, g), typical of perennial, hydrophytic to helophytic aquatic herbs.

Leaf impressions, abundant stems, roots, and tree branch parts are also found in this layer, with lengths reaching 25 cm, some of these related to angiosperm taxa with attached petiolate dicot leaves (Fig. 3, h). These suggest an autochthonous to parautochthonous deposition (*sensu*[81]) with virtually *in situ* or no distant source, especially in the riparian elements of the flora (i.e. Typhaceae and Equisetaceae).

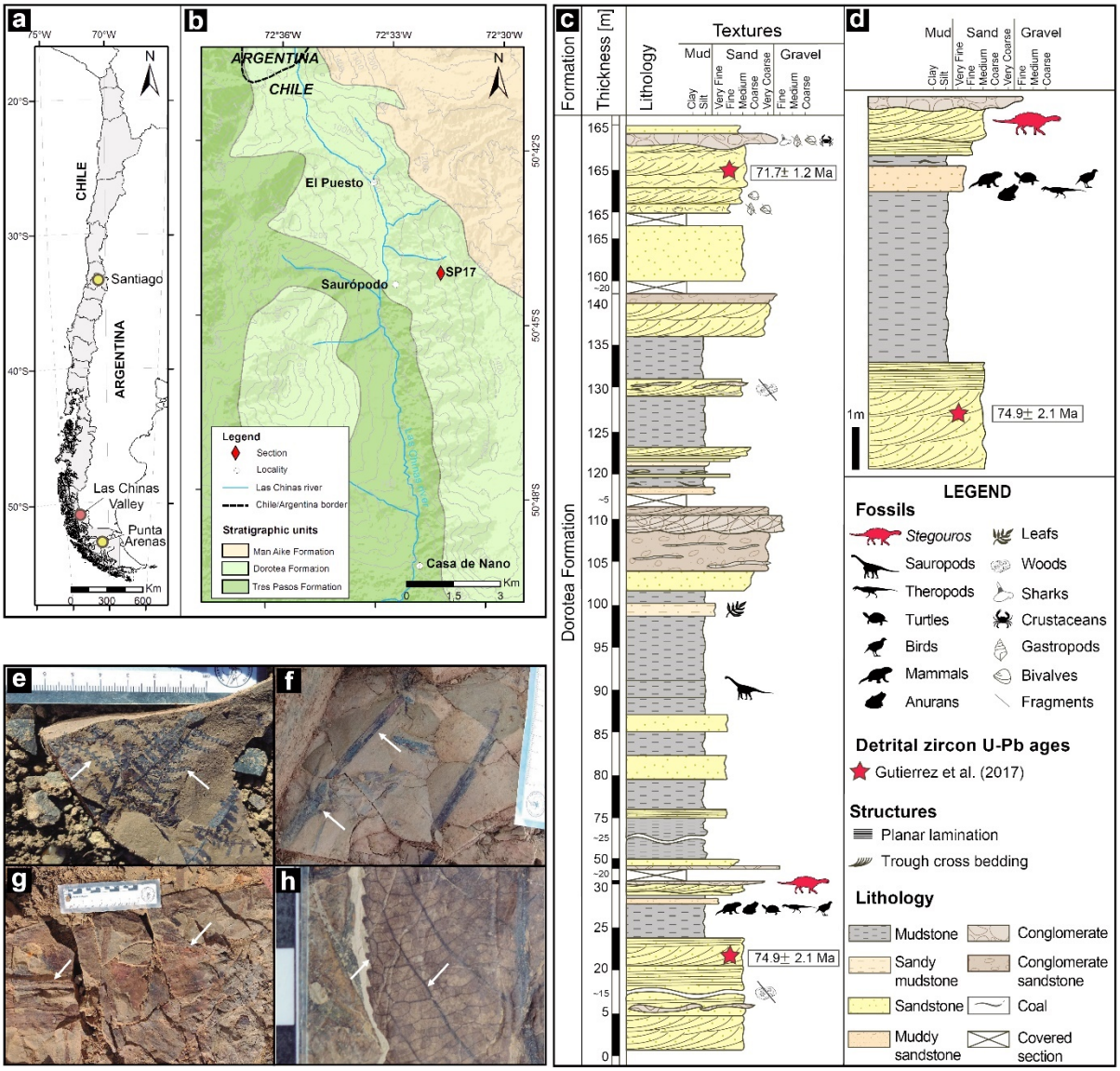

Supplementary Fig.3 Location and stratigraphical context of the finding of *Stegouros elengassen* holotype. **a,** Map of Chile highlighting the location of Río de las Chinas Valley in Chilean Patagonia. **b,** Areal distribution of the Magallanes Basin formations in the sector of Rio de las Chinas Valley, with the studied locality (SP17). **c,** General stratigraphic column of 'Sauropodo sector'. **d,** detail section showing the fossiliferous horizon. **e-h**, In-situ plant fossil outcrops at Saurópodo locality. **e,** Sterile and fertile fern pinnae. Arrows indicate reproductive structures. **f,** Tree branch with an attached angiosperm leaf. **g,** Large leaf assigned to Typhaceae. Arrows indicate the wide leaf midrib. **h,** Very well-preserved large dicot leaf of indeterminate affinity. Arrows indicate areolation and tooth venation.

3. Additional comparisons of *Stegouros elengassen* with *Antarctopelta oliveroi*

Besides the comparisons mentioned in the main text, our direct examination of *Antarctopelta oliveroi* MLP 86-X-28-1 and *Stegouros* revealed other similarities. In both, the cervical centra have concave lateral surfaces (a character usually found in Stegosauria[15], and the first dorsosacral centrum has an expanded border in the anterior articular face, which has previously been described as an unusual feature for an ankylosaur[3] (but see[29,82]). The morphology of anterior and posterior caudal vertebrae of *Stegouros* is similar to proposed homologous elements of MLP 86-X-28 according to[7]. A proximal caudal vertebra of MLP 86-X-28 has been argued to be a pygal (anterior caudal) vertebra of a mosasaur, based on the triangular lateral outline (in cranial view) of a preserved half centrum, and the ventralized position of the transverse process[3]. However, the centra of pygal vertebrae in mosasaurs and other squamates are markedly procoelous[83], whereas the centra of anterior caudals of *Stegouros* also have the roughly triangular lateral outline, and a very similar inclination of the posterior articular surface (Extended Data Fig. 7k). The only notable difference is that the transverse processes in *Antarctopelta* are more ventrally placed. A proposed distal caudal centrum of MLP 86-X-28-1 was also suggested to be a cervical centrum of an elasmosaurian plesiosaur, based on the combined presence of long articulations for the ribs, and the binocular shape ('dumbbell-shape' of[84]) of the centrum[3] (Fig. 10). However, elasmosaur cervical centra bear paired foramina on the ventral surface[85], and the presence of ossified tendons on the ventral surface of the proposed distal caudal centrum of MLP 86-X-28 precludes an assignment to marine reptiles[82]. In turn, this centrum of MLP 86-X-28 resembles the posterior caudals of *Stegouros*, being dorsoventrally compressed (flat), with antero-posteriorly wide transverse process, and a ventral sulcus (Extended Data Fig. 7h-o). The main noticeable difference is that in *Stegouros* ossified tendons are absent. Although appendicular remains of MLP 86-X-28-1 are highly fragmentary, some similarities with *Stegouros* can be noted. Metatarsal IV of both taxa has a laterally expanded proximal epiphysis, with a convex dorsal surface and a slightly concave plantar surface (Extended Data Fig. 7p-t). The preserved diaphyseal portion of metatarsal IV of *Antarctopelta* tapers significantly respect to the epiphysis, which along with an extended contact surface with metatarsal III, suggests a gracile foot as in *Stegouros*, unlike the distally spreading foot of other ankylosaurs and stegosaurs[86,87]. One preserved pedal phalanx in MLP 86-X-28-1 is very flat, similar to the phalanges of toes three and four of *Stegouros* (Extended Data Fig. 7u). Unlike *Kunbarrasaurus* and other Ankylosauria, large osteoderms that encircle the neck are not known for *Stegouros* and *Antarctopelta*. Although this could be a preservation artifact, it is worth noting that such osteoderms are present in *Scelidosaurus* and are likely ancestral for Ankylosauria. If actually absent in *Stegourus* or *Antarctopelta*, this would be a derived condition. MLP 86-X-28-1 also comprises large elements identified as cranial bones by[7] (fig. 3) which have an osteoderm-like texture of pits and striae on their external surface. These were compared by[7] with *Edmontonia*, an ankylosaur whose skull bones are fused to osteoderms[88-90]. However, these elements do not compare well with skull bones of *Kunbarrasaurus*, which are not fused to osteoderms; further,

comparison to *Stegouros* suggests these elements may correspond to osteoderms of the caudal weapon (Extended Data Fig. 8). When compared to the most proximal (1st) pair of large osteoderms of the weapon, the putative supraorbital bone figured by[7] (Fig 3 a, b) shares a strongly concave medial surface, and a dorsal surface that is flatter than the convex ventrolateral surface; both surfaces are separated by a long acuminate keel with a backwardly slanted apex (Extended Data Fig. 8a, d). The element originally identified as a putative parietal bone[7] (Fig 3 d) also bears an internally concave surface and resembles an osteoderm of the second pair in the caudal weapon of *Stegouros*, which is larger and has a flatter dorsal surface (Extended Data Fig. 8e-j).

4. Results of Phylogenetic analyses

In order to resolve the phylogenetic relationships of *Stegouros elengassen*, we carried out five cladistic analyses based on different datasets. The first analysis was made using the data matrix of[22] which is based on 383 characters, consisting of a large sample of ornithischian dinosaurs, including some thyreophorans. The second dataset is a version of the data matrix of[24] modified by[12] which is focused on Stegosauria, comprising 118 characters to which we added 10 new characters. The third dataset used was that of[35], which is an expanded version of the matrix of[3] focused on ankylosauria, originally with 177 characters, to which we added 12 new characters. The fourth analysis was based on the matrix built published by[4], which is focused on Ankylosauria and comprises 295 characters, to which we added 13 new characters. The fifth dataset is from[23] which tests the position of *Scelidosaurus* and includes 115 characters, to which we added 12 new characters. The changes made in the respective data matrices are detailed below. All the data matrices are available as TNT files at doi:10.5061/dryad.pk0p2ngpj

4.1. List of modifications to the data matrix of Han et al.[22]

Character 45 – *Kunbarrasaurus* changed from ? to 1, based on[6].

Character 46 – *Kunbarrasaurus* changed from ? to 0, based on[6].

Character 47 – *Kunbarrasaurus* changed from ? to 1, based on[6].

Character 103 – *Kunbarrasaurus* changed from ? to 1, based on[6].

Character 104 – *Kunbarrasaurus* changed from ? to 0, based on[6].

Character 123 – *Kunbarrasaurus* changed from ? to 0, based on[6].

Character 126 – *Kunbarrasaurus* changed from ? to 0, based on[6].

Character 128 – *Kunbarrasaurus* changed from ? to 0, based on[6].

Character 130 – *Kunbarrasaurus* changed from ? to 0, based on [6].

Character 132 – *Kunbarrasaurus* changed from ? to 2, based on [6].

Character 133 – *Kunbarrasaurus* changed from ? to 0, based on [6].

Character 205 – *Kunbarrasaurus* changed from ? to 1, based on [26].

Character 206 – *Kunbarrasaurus* changed from ? to 0, based on [26].

Character 207 – *Gargoyleosaurus* changed from ? to 0 based on[91]; *Pinacosaurus* changes from 0 to 1 based on[89,91]; *Kunbarrasaurus* changed from 0 to 1, based on[26].

Character 208 – *Gargoyleosaurus* changed from ? to 0 based[91]; *Pinacosaurus* changes from 0 to 1 based on[89,91]; *Kunbarrasaurus* changed from 0 to 1, based onr[26].

Character 214 – *Kunbarrasaurus* changed from ? to 1, based on[26].

Character 219 – *Kunbarrasaurus* changed from ? to 1, based on[26].

Character 220 – *Kunbarrasaurus* changed from ? to 1, based on[26].

Character 224 – *Kunbarrasaurus* changed from ? to 1, based on[26].

Character 252 – Redefinition (new character state added): Distal caudal centra, proportions: length greater than width and height (0), lenght subequal to width and height (1), length subequal to width but greater than height ("flat" centrum) (2)

Character 253 – *Kunbarrasaurus* changed from 2 to ?, based on[26].

Character 256 – *Kunbarrasaurus* changed from ? to 1, based on[26,27].

Character 257 – *Kunbarrasaurus* changed from ? to 1, based on[26,27].

Character 258 – *Kunbarrasaurus* changed from ? to 0, based on [26,27].

Character 270 – *Kunbarrasaurus* changed from ? to 0, based on[26].

Character 281 – *Kunbarrasaurus* changed from ? to 1, on[26].

Character 305 – *Kunbarrasaurus* changed from 1 to ?, based on on[26].

Character 381 (NEW) - Form of pelvic osteoderms: no osteoderms (0) unfused, but tightly interlocking osteoderms (1), coossified osteoderm rosettes (2), coossified evenly-sized polygons of similar size (3), coosified irregular osteoderms into a thin sheet-like sacral shield, forming a bony bridge between de sacral spines and the ilium (4)[92]: 140

Character 382 (NEW) - Osteoderms on limbs: absent (0), present on the proximal limbs segments (1), present on proximal and distal limb segments (2)[3]: 166.

Character 383 (NEW) - Shape and texture of millimeter-sized ossicles: amorphous or polygonal ossicles with irregular texture (0), oblate spheroid to squared ossicles with conspicuous orthogonal fibers on the inner surface (1).

4.2. List of modifications to the data matrix of Raven & Maidment[24]

The taxa *Adratiklit bouhlafa*, following[33], *Antarctopelta oliveroi*, *Kunbarrasaurus ieversi* and *Stegouros elengassen* were added to this matrix.

Character 2 - *Scelidosaurus* recorded from ? to 18. Based on description by[93].

Character 27 - *Lesothosaurus* changed from 0 to 1, based on[94]; *Scelidosaurus* changed from ? to 1 based on[93]; *Huayangosaurus* changed from 1 to 0 based on[12,95] where the description in the text does not coincide with coding in the matrix.

Character 29 - The row of encoded taxa published by[12] is switched with that of character 30. This was corrected keeping the order of the character list.

Character 30 - The state of the characters published by[12] is inverted, it was corrected keeping the order as follows: Striation continues with denticles do not extend to cingulum (0); striations extend to cingulum (1). *Lesothosaurus* is recorded from 1 to 0, based on[94]; *Scutellosaurus* changed from 1 to 0 based on[96]; *Kentrosaurus* changed from? a 1 based on [12,97]

Character 53 - *Kentrosaurus* changed from 1 to 0 based on[12]; *Hesperosaurus* changed from? a 0 based on[98]; *Gastonia* changed from? a 1 based on[99]. *Sauropelta* changed from 1 to 0 based on[100].

Character 53 - *Kentrosaurus* changed from ? to 1 based on[97]; *Hesperosaurus* changed from ? to 0 based on[98]; *Gastonia* changed from? to 0 based on[99].

Character 80 - A new character state was added : 2, Equally long as wide but low in height ("flat" morphology) . *Alcovasaurus* changed from 0 to 1 based on[101].

Character 102 - *Sauropelta* changed from 0 to [0 1] based on[102,103,87]; *Euoplocephalus* changed from 2 to 1 based on[56,87].

Character 122 (NEW) - Position of the caudal end of the maxillary tooth row relative to the rostral border of the orbit: posterior (0), anterior or just below (1).

Character 123 (NEW) - Sacrum, number of fused sacrodorsals in the presacral rod: (0) fused sacrodorsals absent; (1) 1 or 2 sacrodorsals; (2) 3 sacrodorsals ; (3) 4 fused sacrodorsals (4) 5 or more fused sacrodorsals .

Character 124 (NEW) - Sacrum, number of fused sacrocaudal incorporated in the synsacrum : (0) no sacrocaudals ; (1) 1 or more sacrocaudals.

Character 125 (NEW) - Presence of a longitudinal ventral concavity or sulcus in mid-posterior caudal vertebrae: absent (0); present (1).

Character 126 (NEW) - Manual digit II phalangeal formula: three phalanges (0); two or less phalanges (1).

Character 127 (NEW) - Pedal digit II, phalangeal formula: three phalanges (0); two or fewer phalanges (1).

Character 128 (NEW) - Side trunk keeled scutes or osteoderms, over the rib cage: present (0); absent (1).

Character 129 (NEW) - Form of pelvic osteoderms: no osteoderms (0) unfused, but tightly interlocking osteoderms (1), coossified osteoderm rosettes (2), coossified evenly-sized polygons of similar size (3), coosified irregular osteoderms into a thin sheet-like sacral shield, forming a bony bridge between de sacral spines and the ilium (4) [92]: 140.

Character 130 (NEW) - Osteoderms on limbs: absent (0), present on the proximal limbs segments (1), present on proximal and distal limb segments (2)[35]: 166.

Character 131 (NEW) - Shape and texture of millimeter-sized ossicles: amorphous or polygonal ossicles with irregular texture (0), oblate spheroid to squared ossicles with conspicuous orthogonal fibers on the inner surface (1).

4.3. List of modifications to the data matrix of Arbour and Currie[3].

New taxa added are *Paranthodon africanus*[12], *Zuul cruravastator*[104], *Jinyunpelta sinensis*[105], *Borealopelta markmitchelli*[106], *Akainacephalus johnsoni*[4,107], *Antarctopelta oliveroi*[7] and *Stegouros elengassen*.

Character 15 - *Tsagantegia longicranialis* changed from 1 to 0 according to[107].

Character 103 - Salitral Moreno (Argentinean) ankylosaur changed from 1 year, since the specimen does not preserve sacral vertebrae[108].

Character 115 - *Hylaeosaurus* changed from 1 to 0 based on[109].

Character 156 - *Kunbarrasaurus* changed from 1 to [1 2] based on[27].

Character 166 - A new state was added: 2, present on proximal ans distal limb segments (2).

Character 168 - *Kunbarrasaurus* changed from 2 to 1, based on[27]

Character 170 - *Kunbarrasaurus* changed from 2 to 1, based on[27].

Character 171 - *Kunbarrasaurus* changed from? to 0, based on[27].

Character 172 - A new state was added: 4, Coosified irregular osteoderms into a thin sheet-like sacral shield, forming a bony bridge between de sacral spines and the ilium.

Character 178 (NEW) - Caudal end of maxillary tooth row relative position to the rostral border of the orbit: caudal (0), rostral to or just below (1).

Character 179 (NEW) - Tooth crowns: asymmetric (0); symmetric (1).

Character 180 (NEW) - Tooth crowns: do not extend to cingulum (0); striations extend to cingulum (1).

Character 181 (NEW) - Tooth crowns: striations not confluent with denticles (0); confluent with denticles (1).

Character 182 (NEW) - Sacrum, number of fused sacrodorsals in the presacral rod: (0) fused sacrodorsals absent; (1) 1 or 2 sacrodorsals ; (2) 3 sacrodorsals ; (3) 4 fused sacrodorsals (4) 5 or more fused sacrodorsals .

Character 183 (NEW) - Sacrum, number of fused sacrocaudal incorporated in the synsacrum: (0) no sacrocaudals; (1) 1 or more sacrocaudals.

Character 184 (NEW) - Presence of a longitudinal ventral groove or sulcus in mid to posterior caudal vertebrae (haemal canal): absent (0); present (1).

Character 185 (NEW) - Posterior caudal vertebrae: centra are elongate (0); equidimensional (length, height and width roughly equivalent) (1); Equally long as wide but low in height ("flat") (2).

Character 186 (NEW) - Humerus: triceps tubercle and descending ridge posterolateral to the deltopectoral crest: absent (0), present (1)[17,24].

Character 187 (NEW) - Manual digit II phalangeal formula: three phalanges (0); two or less phalanges (1).

Character 188 (NEW) - Pedal digit II, phalangeal formula: three phalanges (0); two or fewer phalanges (1).

Character 189 (NEW) - Shape and texture of millimeter-sized ossicles: amorphous or polygonal ossicles with irregular texture (0), oblate spheroid to squared ossicles with conspicuous orthogonal fibers on the inner surface (1).

4.4. List of modifications to the data matrix of Loewen and Kirkland[4, 25]

The taxa *Stegouros elengassen*, *Antarctopelta oliveroi* and *Isaberrysaura mollensis* were added to this matrix. The taxon '*Tarchia gigantea'* (originally *Dyoplosaurus giganteus*[110], was removed, as the holotype consists of a fragmentary postcranium lacking autapomorphies[3]. Also, the PIN 3142/250 specimen, on which the coding of '*Tarchia gigantea'* is based in part, was referred to *Saichania chulsanensis* by[3], but later designated as a holotype of *Tarchia teresae* by[111].

The following taxa included in this analysis have been synonymized in recent reviews: *Zhongyuansaurus lauyangensis*, considered a junior synonym of *Gobisaurus domuculus*[3]; *Tianzhenosaurus youngi*, considered as a junior synonym of *Saichania chulsanensis*[3]; *Shanxia tianzhenensis*, considered as a junior synonym of *Saichania chulsanensis*[3]; *Minotaurasaurus ramachandrani*, considered as a junior synonym of *Tarchia kielanae*[3] (however, see also[107]); *Oohkotokia horneri*, considered as a junior synonym of *Scolosaurus cutleri*[3] (however, see also[112]). However, when removed from the analysis, this did not affect the position and stability of Parankylosauria. We therefore decided to keep them as separate OTUs.

Character 140 – Character state 1 was divided into three states: Sacrum, number of fused sacrodorsals in the presacral rod: fused sacrodorsals absent (0); 1 or 2 sacrodorsals (1); 3 sacrodorsals (2).

Character 141 - *Cedarpelta bilbeyhallorum* changed from 1 to 2 based on[113] ; *Crichtonpelta benxiensis* changed from 1 to 2 based on[114]; *Pinacosaurus mephistocephalus* changed from 2 to 1 based on[115]; *Tianzhenosaurus youngi* changed from 2 to 1 based on[116], *Scolosaurus cutleri* changed from 1 to 2 based on[117]; *Anodontosaurus lambei* changed from 1 to 2 based on; *Oohkotokia horneri* changed from

1 to 2 based on[112]; *Euoplocephalus tutus* changed from 1 to 2 based on[112,118]; *Dyoplosaurus acutosquameus* changed from 1 to 2 based on[112,119,120].

Character 260 - A new state was added to the character: Thin sacral shield composed covering just the space between ilia and sacral spines (3). It was treated as unordered.

Character 293 - *Kunbarrasaurus* changed from 0 to ?, since the distal end of the tail is unknown[26,27].

Character 294 (NEW) - Caudal end of maxillary tooth row relative position to the rostral border of the orbit: caudal (0), rostral to or just below (1).

Character 295 (NEW) - Tooth crowns: asymmetric (0); symmetric (1).

Character 206 (NEW) - Tooth crowns: do not extend to cingulum (0); striations extend to cingulum (1).

Character 297 (NEW) - Tooth crowns: striations not confluent with denticles (0); confluent with denticles (1).

Character 298 (NEW) - Sacrum, number of fused sacrocaudal incorporated in the synsacrum: (0) no sacrocaudals; (1) 1 or more sacrocaudals.

Character 299 (NEW) - Presence of a longitudinal ventral groove or sulcus in mid to posterior caudal vertebrae (haemal canal): absent (0); present (1).

Character 300 (NEW) - Posterior caudal vertebrae: centra are elongate (0); equidimensional (length, height, and width roughly equivalent) (1); Equally long as wide but low in height ("flat") (2)

Character 301 (NEW) - Humerus: triceps tubercle and descending ridge posterolateral to the deltopectoral crest: absent (0), present (1)[17,24].

Character 302 (NEW) - Manual digit II phalangeal formula: three phalanges (0); two or less phalanges (1).

Character 303 (NEW) - Pedal digit II, phalangeal formula: three phalanges (0); two or fewer phalanges (1).

Character 304 (NEW) - Osteoderms on limbs: absent (0), present on the proximal limbs segments (1), present on proximal and distal limb segments (2) (modified from[3]).

Character 305 (NEW) - Osteoderms: mosaic of small osteoderms between larger osteoderms on the ventral surfaces of the neck, trunk, and proximal portions of the limbs absent (0); present (1).

Character 306 (NEW) - Shape and texture of millimeter -sized ossicles: amorphous or polygonal ossicles with irregular texture (0), oblate spheroid to squared ossicles with conspicuous orthogonal fibers on the inner surface (1).

4.5. List of modifications to the data matrix of Norman[23]

The taxa *Antarctopelta oliveroi* and *Stegouros elengassen* were added to the original matrix.

Character 5 - *Kunbarrasaurus* changed from 2 to ?, trait is not preserved in specimen[6,26].

Character 36 - *Kunbarrasaurus* changed from 0 to 1 based on[6].

Character 39 - *Kunbarrasaurus* changed from 2 to ?, predentary is not preserved in specimen[6].

Character 52 - *Kunbarrasaurus* changed from 0 to 2 based on26.

Character 58 - *Huayangosaurus* changed from 0 to 1 based on[121]; *Kentrosaurus* changed from 0 to 1 based on[122]; *Stegosaurus* changed from 0 to 1 based on[123, 124].

Character 110 - Definition of the character was modified: osteoderms on limbs: absent (0), present on limb proximal segments (1) present on proximal and distal limb segments (2) (modified from[35]).

Character 116 (NEW) - Caudal end of maxillary tooth row relative position to the rostral border of the orbit: caudal (0), rostral to or just below (1).

Character 117 (NEW) - Tooth crowns: asymmetric (0); symmetric (1).

Character 118 (NEW) - Tooth crowns: striations not confluent with denticles (0); confluent with denticles (1).

Character 119 (NEW) - Sacrum, number of fused sacrodorsals in the presacral rod: (0) fused sacrodorsals absent; (1) 1 or 2 sacrodorsals; (2) 3 sacrodorsals; (3) 4 fused sacrodorsals (4) 5 or more fused sacrodorsals.

Character 120 (NEW) - Sacrum, number of fused sacrocaudals incorporated in the synsacrum: (0) no sacrocaudals; (1) 1 or more sacrocaudals.

Character 121 (NEW) - Presence of a longitudinal ventral groove or sulcus in mid to posterior caudal vertebrae (haemal canal): absent (0); present (1).

Character 122 (NEW) - Posterior caudal vertebrae: centra are elongate (0); equidimensional (length, height and width roughly equivalent) (1); Equally long as wide but low in height ("flat") (2).

Character 123 (NEW) - Humerus: triceps tubercle and descending ridge posterolateral to the deltopectoral crest: absent (0), present (1).[17,24].

Character 124 (NEW) - Manual digit II phalangeal formula: three phalanges (0); two or less phalanges (1).

Character 125 (NEW) - Pedal digit II, phalangeal formula: three phalanges (0); two or fewer phalanges (1).

Character 126 (NEW) - Millimeter -sized ossicles abundant in spaces between osteoderms in thoracic or caudal regions (excluding pelvic region), absent (0), present (1). [Based on observations presented in[92]].

Character 127 (NEW) - Shape and texture of millimeter -sized ossicles: amorphous or polygonal ossicles with irregular texture (0), oblate spheroid to squared ossicles with conspicuous orthogonal fibers on the inner surface (1).

4.6. Results

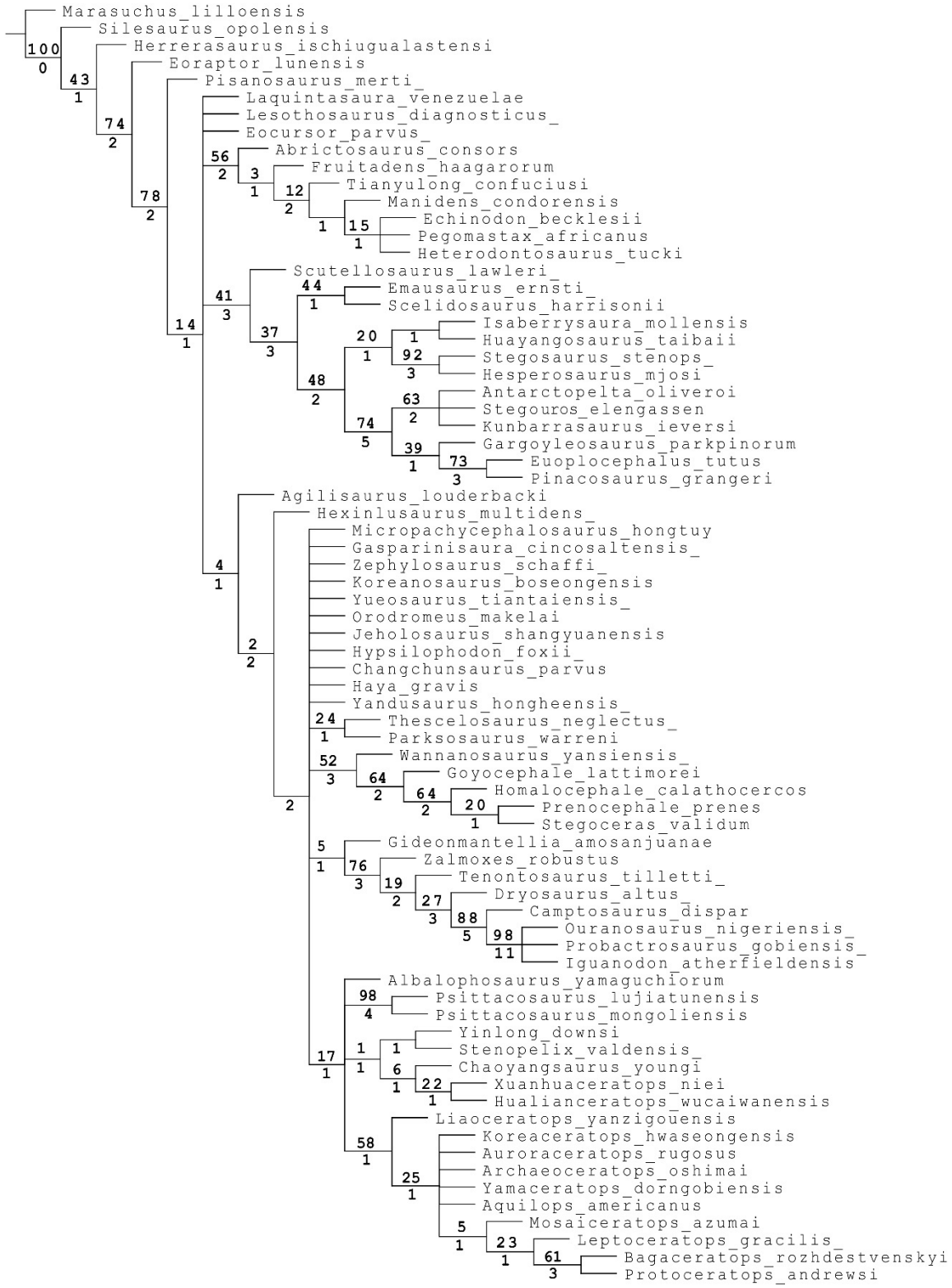

Fig. 4. Strict consensus of 13392 MPTs resulting from analysis of Han et al matrix. Values above nodes represent bootstrap proportions (1000 pseudoreplicates). Values beneath nodes represent Bremmer support.

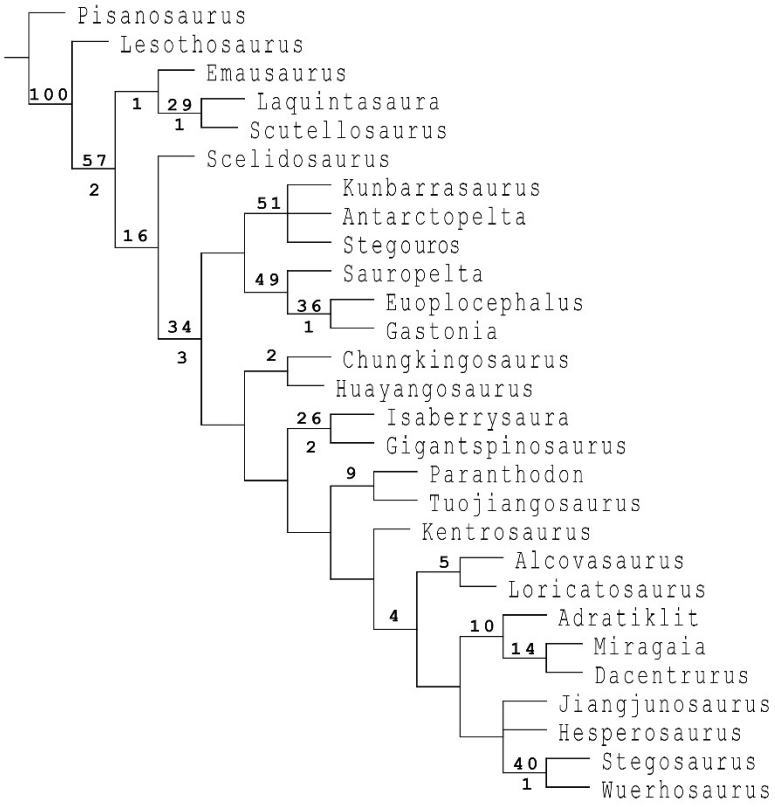

Fig. 5. Strict consensus of 2 MPTs resulting from analysis of Raven and Maidment matrix. Values above nodes represent bootstrap proportions (1000 pseudoreplicates). Values beneath nodes represent Bremmer support.


Lesothosaurus_diagnosticus
Scelidosaurus_harrisonii
Huayangosaurus_taibaii
Stegosaurus_stenops
Paranthodon_africanus
Antarctopelta_oliveroi
Stegouros_elengassen
Kunbarrasaurus_ieversi
Aletopelta_coombsi
Liaoningosaurus_paradoxus
Chuanqilong_chaoyangensis
Gobisaurus_domoculus
Shamosaurus_scutatus
Jinyunpelta_sinensis
Crichtonpelta_benxiensis
Akainacephalus_johnsoni
Zhejiangosaurus_luoyangensis
Zaraapelta_nomadis
Tsagantegia_longicranialis
Tarchia_kielanae
Talarurus_plicatospineus
Scolosaurus_cutleri
Saichania_chulsanensis
Pinacosaurus_mephistocephalus
Pinacosaurus_grangeri
Nodocephalosaurus_kirtlandensis
Zuul_cruravastator
Dyoplosaurus_acutosquameus
Ziapelta_sanjuanensis
Euoplocephalus_tutus
Anodontosaurus_lambei
Ankylosaurus_magniventris
Taohelong_jinchengensis
Sauroplites_scutiger
Hoplitosaurus_marshi
Polacanthus_foxii
Peloroplites_cedrimontanus
Panoplosaurus_mirus
Mymoorapelta_maysi
Hylaeosaurus_armatus
Gastonia_burgei
Gargoyleosaurus_parkpinorum
Dongyangopelta_yangyanensis
Cedarpelta_bilbeyhallorum
Animantarx_ramaljonesi
Texasetes_pleurohalio
Salitral_Moreno_ankylosaur
Edmontonia_longiceps
Edmontonia_rugosidens
Denversaurus_schlessmani
Sauropelta_edwardsi
Tatankacephalus_cooneyorum
Silvisaurus_condrayi
Paw_Paw_scuteling
Niobrarasaurus_coleii
Ahshislepelta_minor
Nodosaurus_textilis
Hungarosaurus_tormai
Europelta_carbonensis
Stegopelta_landerensis
Pawpawsaurus_campbelli
Struthiosaurus_transylvanicus
Borealopelta_markmitchelli
Struthiosaurus_languedocensis
Struthiosaurus_austriacus

Fig. 6. Strict consensus of 20 MPTs resulting from analysis of Arbour et al matrix. Values above nodes represent bootstrap proportions (1000 pseudoreplicates). Values beneath nodes represent Bremmer support.

Fig. 7. Strict consensus of 16 MPTs resulting from analysis of Loewen and Kirkland matrix. Values above nodes represent bootstrap proportions (1000 pseudoreplicates). Values beneath nodes represent Bremmer support.

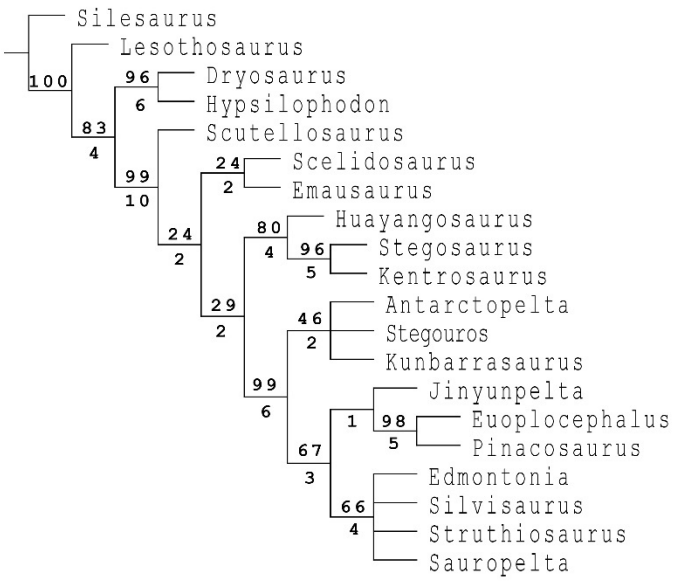

Fig. 8. Strict consensus of 4 MPTs resulting from analysis of Norman matrix. Values above nodes represent bootstrap proportions (1000 pseudoreplicates). Values beneath nodes represent Bremmer support.

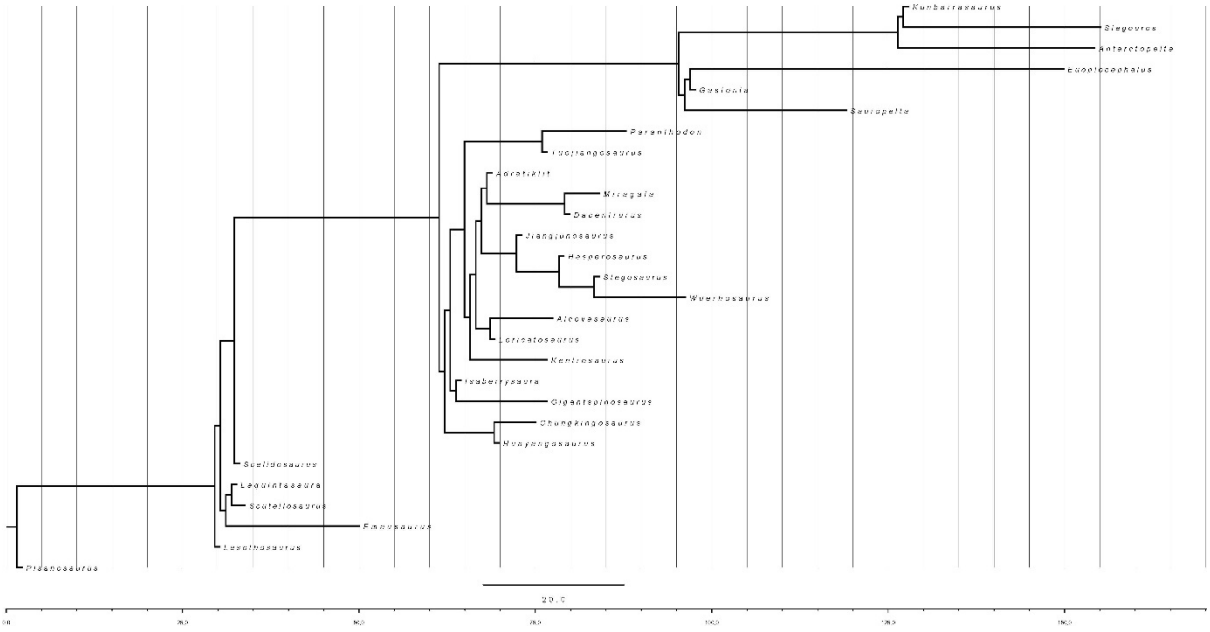

Fig. 9. Time-calibrated subtree from analysis of Raven and Maidment matrix. Subtree number 2.

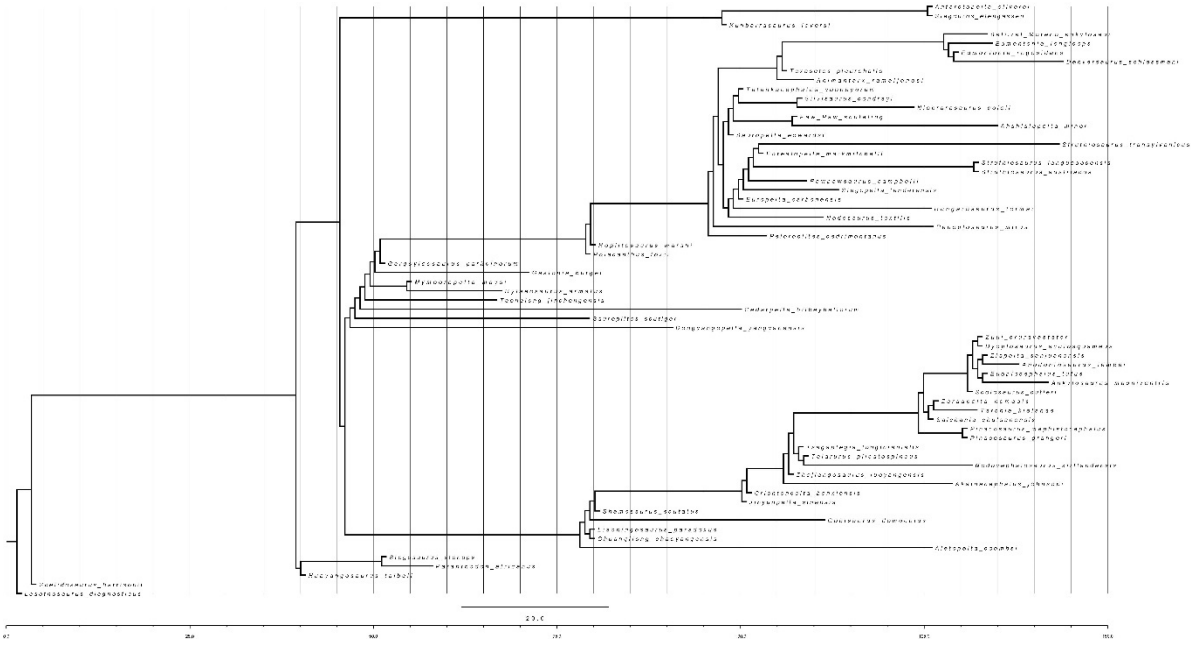

Fig. 10. Time-calibrated subtree from analysis of Arbour et al matrix. Subtree number 1.

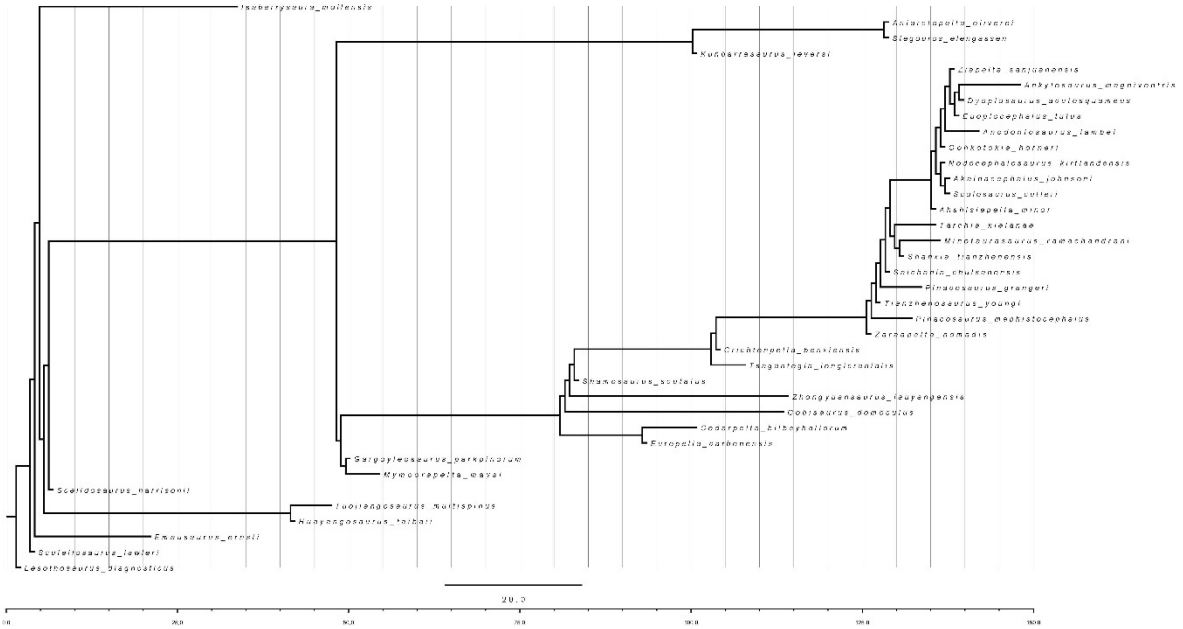

Fig. 11. Time-calibrated subtree from analysis of Loewen and Kirkland matrix. Subtree number 1.

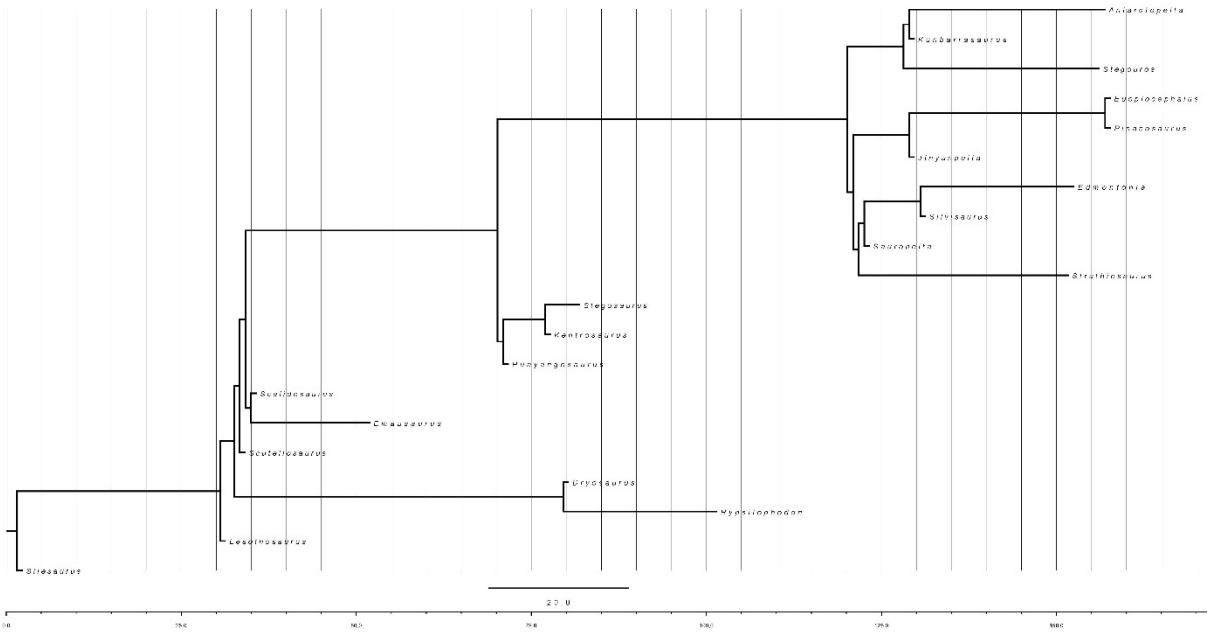

Fig. 12. Time-calibrated subtree from Norman matrix. Subtree number 2.

4.7. Data for the calculation of the modified MSM or the GER

Age character matrix for the calculation of the modified MSM or the GER (Raven & Maidment matrix)

Pisanosaurus	1
Lesothosaurus	2
Scutellosaurus	3
Emausaurus	4
Scelidosaurus	3
Huayangosaurus	8
Dacentrurus	9
Miragaia	A
Loricatosaurus	7
Kentrosaurus	9
Chungkingosaurus	9

Tuojiangosaurus 9

Gigantspinosaurus 9

Wuerhosaurus C

Stegosaurus A

Hesperosaurus 9

Gastonia D

Sauropelta E

Euoplocephalus G

Jiangjunosaurus 8

Laquintasaura 2

Alcovasaurus 9

Adratiklit 6

Isaberrysaura 5

Paranthodon B

Stegouros H

Antarctopelta H

Kunbarrasaurus F

set age[0] 237;

set age[1] 229;

set age[2] 201;

set age[3] 199;

set age[4] 182;

set age[5] 170;

set age[6] 168;

set age[7] 166;

set age[8] 163;

set age[9] 157;

set age[10] 152;

set age[11] 145;

set age[12] 139;

set age[13] 136;

set age[14] 113;

set age[15] 105;

set age[16] 83;

set age[17] 77;

Age character matrix for the calculation of the modified MSM or the GER (Arbour & Currie matrix)

Lesothosaurus_diagnosticus	1
Scelidosaurus_harrisonii	2
Huayangosaurus_taibaii	3
Paranthodon_africanus	6
Stegosaurus_stenops	5
Ahshislepelta_minor	I
Akainacephalus_johnsoni	I
Aletopelta_coombsi	I
Animantarx_ramaljonesi	D
Ankylosaurus_magniventris	K

Anodontosaurus_lambei	J
Borealopelta_markmitchelli	B
Cedarpelta_bilbeyhallorum	C
Chuanqilong_chaoyangensis	A
Crichtonpelta_benxiensis	C
Denversaurus_schlessmani	K
Dongyangopelta_yangyanensis	B
Dyoplosaurus_acutosquameus	I
Edmontonia_rugosidens	H
Edmontonia_longiceps	I
Euoplocephalus_tutus	I
Europelta_carbonensis	B
Gargoyleosaurus_parkpinorum	4
Gastonia_burgei	8
Gobisaurus_domoculus	E
Hungarosaurus_tormai	G
Hylaeosaurus_armatus	7
Jinyunpelta_sinensis	C
Liaoningosaurus_paradoxus	A
Mymoorapelta_maysi	5
Niobrarasaurus_coleii	F
Nodocephalosaurus_kirtlandensis	I
Nodosaurus_textilis	D
Panoplosaurus_mirus	H

Paw_Paw_scuteling	C
Pawpawsaurus_campbelli	C
Peloroplites_cedrimontanus	C
Pinacosaurus_grangeri	I
Pinacosaurus_mephistocephalus	I
Polacanthus_foxii	9
Hoplitosaurus_marshi	9
Saichania_chulsanensis	H
Sauropelta_edwardsi	B
Sauroplites_scutiger	A
Scolosaurus_cutleri	I
Shamosaurus_scutatus	A
Silvisaurus_condrayi	C
Stegopelta_landerensis	D
Struthiosaurus_austriacus	H
Struthiosaurus_languedocensis	H
Struthiosaurus_transylvanicus	J
Talarurus_plicatospineus	D
Taohelong_jinchengensis	7
Tarchia_kielanae	I
Tatankacephalus_cooneyorum	B
Texasetes_pleurohalio	C
Tsagantegia_longicranialis	D
Zaraapelta_nomadis	H

Zhejiangosaurus_luoyangensis	D
Ziapelta_sanjuanensis	I
Zuul_cruravastator	I
Salitral_Moreno_ankylosaur	I
Kunbarrasaurus_ieversi	C
Stegouros_elengassen	I
Antarctopelta_oliveroi	I

set age[0] 205;

set age[1] 201;

set age[2] 199;

set age[3] 163;

set age[4] 157;

set age[5] 152;

set age[6] 145;

set age[7] 139;

set age[8] 136;

set age[9] 129;

set age[10] 125;

set age[11] 113;

set age[12] 105;

set age[13] 100;

Age character matrix for the calculation of the modified MSM or the GER (Loewen & Kirkland matrix)

Lesothosaurus_diagnosticus	1
Scutellosaurus_lawleri	2
Emausaurus_ernsti	3
Huayangosaurus_taibaii	5
Tuojiangosaurus_multispinus	6
Scelidosaurus_harrisonii	2
Mymoorapelta_maysi	7
Gargoyleosaurus_parkpinorum	6
Europelta_carbonensis	9
Cedarpelta_bilbeyhallorum	A
Gobisaurus_domoculus	C
Zhongyuansaurus_lauyangensis	C
Shamosaurus_scutatus	8
Tsagantegia_longicranialis	B
Crichtonpelta_benxiensis	A
Zaraapelta_nomadis	D
Pinacosaurus_mephistocephalus	E
Tianzhenosaurus_youngi	D
Pinacosaurus_grangeri	E
Saichania_chulsanensis	D
Ahshislepelta_minor	E
Scolosaurus_cutleri	E

Shanxia_tianzhenensis	D
Akainacephalus_johnsoni	E
Nodocephalosaurus_kirtlandensis	E
Minotaurasaurus_ramachandrani	E
Tarchia_kielanae	E
Anodontosaurus_lambei	F
Oohkotokia_horneri	E
Euoplocephalus_tutus	E
Dyoplosaurus_acutosquameus	E
Ankylosaurus_magniventris	G
Ziapelta_sanjuanensis	E
Kunbarrasaurus_ieversi	A
Stegouros_elengassen	E
Antarctopelta_oliveroi	E
Isaberrysaura_mollensis	4

set age[0] 205;

set age[1] 201;

set age[2] 199;

set age[3] 182;

set age[4] 170;

set age[5] 163;

set age[6] 157;

set age[7] 152;

set age[8] 125;

set age[9] 113;

set age[10] 105;

set age[11] 100;

set age[12] 93;

set age[13] 83;

set age[14] 77;

set age[15] 72;

set age[16] 68;

Age character matrix for the calculation of the modified MSM or the GER (Norman matrix)

Pisanosaurus	1
Lesothosaurus	2
Scutellosaurus	3
Emausaurus	4
Scelidosaurus	3
Huayangosaurus	8
Dacentrurus	9
Miragaia	A
Loricatosaurus	7
Kentrosaurus	9
Chungkingosaurus	9
Tuojiangosaurus	9
Gigantspinosaurus	9

Wuerhosaurus	C
Stegosaurus	A
Hesperosaurus	9
Gastonia	D
Sauropelta	E
Euoplocephalus	G
Jiangjunosaurus	8
Laquintasaura	2
Alcovasaurus	9
Adratiklit	6
Isaberrysaura	5
Paranthodon	B
Stegouros	H
Antarctopelta	H
Kunbarrasaurus	F

set age[0] 237;

set age[1] 229;

set age[2] 201;

set age[3] 199;

set age[4] 182;

set age[5] 170;

set age[6] 168;

set age[7] 166;

set age[8] 163;

set age[9] 157;

set age[10] 152;

set age[11] 145;

set age[12] 139;

set age[13] 136;

set age[14] 113;

set age[15] 105;

set age[16] 83;

set age[17] 77;

Supplementary Table II: Selected postcranial measurements of the holotype of *Stegouros elengassen* gen. et sp. nov

Bone	Total lenght	Proximal width	Distal width	Bone	Total lenght	Proximal width	Distal width
Left humerus	158,00	-	57,00	Right metacarpal I	33,90	16,00	12,10
Left radius	105,50	20,20	31,90	Right phalanx I-1	14,40	13,60	-
Left ulna	120,70	41,30	27,80	Right phalanx I-2	18,70	-	-
Left metacarpal I	34,20	15,60	13,90	Right metacarpal II	39,20	14,20	14,50
Left metacarpal II	37,50	16,20	15,20	Right phalanx II-1	11,20	11,60	-
Left metacarpal III	34,40	19,90	16,30	Right phalanx II-2	19,80	-	-
Left metacarpal IV	28,10	13,30	11,50	Right ilium	241*		

Left metacarpal V	19,30	11,80	10,00	Right ischium	157,00	59,30	
Left ilium	275,00			Right femur	163,00	47,20	52,70
Left ischium	141*	54,40		Right tibia	-	54,40	57,10
Left femur	150,60	47,70	51,50	Right metatarsal I	36,50		
Left tibia	144,90	58,70	51,50	Right phalanx I-1	16,40		
Left metatarsal I	35,00	-	-	Right phalanx I-2	20,60		
Left phalanx I-1	15,60	-	-	Right metatarsal II	68,90		
Left phalanx I-2	20,10	-	-	Right phalanx II-1	24,00		
Left metatarsal II	59,90	-	-	Right phalanx II-2	13,40		
Left phalanx II-1	23,20	-	-	Right phalanx II-3	25,50		
Left phalanx II-2	14,20	-	-	Right metatarsal III	72,80		
Left phalanx II-3	22,40	-	-	Right phalanx III-1	19,60		
Left metatarsal III	70,10	-	-	Right phalanx III-2	12,50		
Left phalanx III-1	20,10	-	-	Right phalanx III-3	9,30		
Left phalanx III-2	12,40	-	-	Right phalanx III-4	29,70		
Left phalanx III-3	10,20	-	-	Right metatarsal IV	65,90	24,07	17,00

Left phalanx III-4	16,2*	-	-	Right phalanx IV-1	21,20
Left metatarsal IV	59,10	20,86	15,70	Right phalanx IV-2	9,00
Left phalanx IV-1	12,40			Right phalanx IV-3	6,50
Left phalanx IV-2	9,80			Right phalanx IV-4	5,50
Left phalanx IV-3	7,00			Right phalanx IV-5	21,5*
Left phalanx IV-4	6,00			Right metatarsal V	23,10
Left phalanx IV-5	19,10				

References:

42 Hammer, O., Harper, D. A. T. & Ryan, P. D. PAST: paleontological statistics software package for education and data analysis palaeontologia electronica. http://palaeo-electronicaorg/2001_1/past/issue1_01htm *Accessed* **4**, 9 (2001).

43 Voorhies, M. R. Taphonomy and population dynamics of an early Pliocene vertebrate fauna, Knox County, Nebraska. *Contributions to Geology* **1**, 1-69 (1966).

44 Behrensmeyer, A. K. The taphonomy and paleoecology of Plio-Pleistocene vertebrate assemblages east of Lake Rudolf, Kenya. *Bull Mus Comp Zool* **146** (1975).

45 Wood, J. M., Thomas, R. G. & Visser, J. Fluvial processes and vertebrate taphonomy: the upper cretaceous Judith River formation, south-central dinosaur Provincial Park, Alberta, Canada. *Palaeogeography, Palaeoclimatology, Palaeoecology* **66**, 127-143 (1988).

46 Holz, M. & Barberena, M. C. Taphonomy of the south Brazilian Triassic paleoherpetofauna: pattern of death, transport and burial. *Palaeogeography, Palaeoclimatology, Palaeoecology* **107**, 179-197 (1994).

47 Kaufmann, C., Gutiérrez, M. A., Álvarez, M. C., González, M. E. & Massigoge, A. Fluvial dispersal potential of guanaco bones (Lama guanicoe) under controlled experimental conditions: the influence of age classes to the hydrodynamic behavior. *J Archaeol Sci* **38**, 334-344 (2011).

48 Mallon, J. C., Henderson, D. M., McDonough, C. M. & Loughry, W. A "bloat-and-float" taphonomic model best explains the upside-down preservation of ankylosaurs. *Palaeogeography, palaeoclimatology, palaeoecology* **497**, 117-127 (2018).

49 Weigelt, J. *Recent vertebrate carcasses and their paleobiological implications*. University of Chicago Press, Chicago (1989).

50 Wilson, T. J. Transition from back-arc to foreland basin development in the southernmost Andes: Stratigraphic record from the Ultima Esperanza District, Chile. *Geol Soc Am Bull* **103**, 98-111 (1991).

51 Fildani, A., Cope, T. D., Graham, S. A. & Wooden, J. L. Initiation of the Magallanes foreland basin: Timing of the southernmost Patagonian Andes orogeny revised by detrital zircon provenance analysis. *Geology* **31**, 1081-1084 (2003).

52 Biddle, K., Uliana, M., Mitchum Jr, R., Fitzgerald, M. & Wright, R. The stratigraphic and structural evolution of the central and eastern Magallanes Basin, southern South America. *Foreland basins*, 41-61 (1986).

53 Mella, P. *Control tectónico en la evolución de la Cuenca de Antepaís de Magallanes, XII Región, Chile* Memoria para optar al título de geólogo, Thesis, Universidad de Concepción (2001).

54 Romans, B. W., Hubbard, S. M. & Graham, S. A. Stratigraphic evolution of an outcropping continental slope system, Tres Pasos Formation at Cerro Divisadero, Chile. *Sedimentology* **56**, 737-764 (2009).

55 Hubbard, S. M., Fildani, A., Romans, B. W., Covault, J. A. & McHargue, T. R. High-relief slope clinoform development: insights from outcrop, Magallanes Basin, Chile. *Journal of Sedimentary Research* **80**, 357-375 (2010).

56 Auchter, N. C., Romans, B. W. & Hubbard, S. M. Influence of deposit architecture on intrastratal deformation, slope deposits of the Tres Pasos Formation, Chile. *Sediment Geol* **341**, 13-26 (2016).

57 Daniels, B. G. *et al.* Timing of deep-water slope evolution constrained by large-n detrital and volcanic ash zircon geochronology, Cretaceous Magallanes Basin, Chile. *Bulletin* **130**, 438-454 (2018).

58 Schwartz, T. M., Fosdick, J. C. & Graham, S. A. Using detrital zircon U-Pb ages to calculate Late Cretaceous sedimentation rates in the Magallanes-Austral basin, Patagonia. *Basin Research* **29**, 725-746 (2016).

59 George, S. W. *et al.* Chronology of deposition and unconformity development across the Cretaceous–Paleogene boundary, Magallanes-Austral Basin, Patagonian Andes. *J South Am Earth Sci* **97**, 102237 (2020).

60 Malumián, N. Foraminíferos de la Formación Man Aike (Eoceno, sureste Lago Cardiel) provincia de Santa Cruz. *Rev Asoc Geol Argent* **45**, 365-385 (1990).
61 Camacho, H. H., Chiesa, J. O., Parma, S. G. & Reichler, V. A. Invertebrados marinos de la Formación Man Aike (Eoceno medio), Provincia de Santa Cruz, Argentina. (2000).
62 Marenssi, S. A., Casadío, S. & Santillana, S. N. Estratigrafía y sedimentología de las unidades del Cretácico superior-Paleógeno aflorantes en la margen sureste del lago Viedma, provincia de Santa Cruz, Argentina. *Rev Asoc Geol Argent* **58**, 403-416 (2003).
63 Schwartz, T. M. & Graham, S. A. Stratigraphic architecture of a tide-influenced shelf-edge delta, Upper Cretaceous Dorotea Formation, Magallanes-Austral basin, Patagonia. *Sedimentology* **62**, 1039-1077 (2015).
64 Sickmann, Z. T., Schwartz, T. M. & Graham, S. A. Refining stratigraphy and tectonic history using detrital zircon maximum depositional age: an example from the Cerro Fortaleza Formation, Austral Basin, southern Patagonia. *Basin Research* **30**, 708-729 (2018).
65 Katz, H. R. Revision of Cretaceous stratigraphy in Patagonian Cordillera of Ultima Esperanza, Magallanes Province, Chile. *AAPG Bulletin* **47**, 506-524 (1963).
66 Covault, J. A., Romans, B. W. & Graham, S. A. Outcrop expression of a continental-margin-scale shelf-edge delta from the Cretaceous Magallanes Basin, Chile. *Journal of Sedimentary Research* **79**, 523-539 (2009).
67 Vogt, M. *et al.* in *23rd Latin American Colloquium on Earth Sciences.* 56 (Talk Heildelberg).
68 Otero, R. A. *et al.* Neoselachians and Chimaeriformes (Chondrichthyes) from the latest Cretaceous–Paleogene of Sierra Baguales, southernmost Chile. Chronostratigraphic, paleobiogeographic and paleoenvironmental implications. *J South Am Earth Sci* **48**, 13-30 (2013).
69 Jujihara, T. *et al.* in *The 23rd Latin American Colloquium on Earth Sciences, Abstracts with Program* (2014).
70 Soto-Acuña, S. *et al.* in *IV Simposio Paleontología en Chile. Universidad Austral de Chile, Valdivia, Abstracts in Program* (2014).
71 Otero, R. A., Salazar C.S., Yury-Yáñez, R., Soto-Acuña, S. & Oyarzún, J. L. New elasmosaurids (Plesiosauria, Sauropterygia) from the Upper Cretaceous of the Magallanes Basin, Chilean Patagonia: Evidence of a faunal turnover during the Maastrichtian along the Weddellian Biogeographic Province. *Andean Geology* **42**, 237-267 (2015).
72 Soto-Acuña, S., Otero, R. A. & Rubilar-Rogers, D. First record of mosasaurs (Lepidosauria: Mosasauridae) from the Late Cretaceous (Maastrichtian) of the Magallanes Basin. *Boletín del Museo Nacional de Historia Natural, Chile* **64**, 69-79 (2015).
73 Suazo Lara, F. *et al.* in *Congreso Chileno de Paleontología.* 331-333 (2018).

74 Goin, F. J. *et al.* First Mesozoic mammal from Chile: The southernmost record of a Late Cretaceous gondwanatherian. *Bol. Mus. Nac. Hist. Nat. Chile* **69**, 5-31 (2020).
75 Alarcón-Muñoz, J. *et al.* Freshwater turtles (Testudines: Pleurodira) in the Upper Cretaceous of Chilean Patagonia. *J South Am Earth Sci* **102**, 102652 (2020).
76 Martinelli, A. G. *et al.* New cladotherian mammal from southern Chile and the evolution of mesungulatid meridiolestidans at the dusk of the Mesozoic era. *Scientific reports* **11**, 1-18 (2021).
77 Cortés, R. Informe Geológico del área Río Las Chinas–Río Bandurrias (Última Esperanza). *Empresa Nacional del Petróleo, Magallanes, Punta Arenas*, 33 (1964).
78 González, E. J. *Estratigrafía secuencial y sedimentología de la Formación Dorotea (Maastrichtiano), sector Río de las Chinas, Región de Magallanes y Antártica Chilena, Chile (50°S)*, Universidad de Chile, (2015).
79 Trevisan, C., Dutra, T., Wilberger, T., Leppe, M. & Manríquez, L. An austral fern assemblage from the Upper Cretaceous (Campanian) beds of Cerro Guido, Magallanes Basin, Chilean Patagonia. *Cretaceous Res* **106**, 104215 (2020).
80 Ellis, B. *et al. Manual of Leaf Architecture*. (Cornell University Press, 2009).
81 Gastaldo, R. A. in *Palaeobiology II* 312-315 (2001).
82 Rozadilla, S., Aranciaga Rolando, A. & Motta, M. On the validity of the Antarctic ankylosaur *Antarctopelta oliveroi* Salgado & Gasparini (Dinosauria, Ornithischia). *Ameghiniana* **53**, 37 (2015).
83 Estes, R., de Queiroz, K. & Gauthier, J. Phylogenetic relationships within Squamata. *Phylogenetic relationships of the lizard families*, 119-281 (1988).
84 Gasparini, Z., Bardet, N., Martin, J. E. & Fernandez, M. The elasmosaurid plesiosaur *Aristonectes* Cabrera from the latest Cretaceous of South America and Antarctica. *J Vertebr Paleontol* **23**, 104-115 (2003).
85 Welles, S. P. A new species of elasmosaur from the Aptian of Colombia and a review of the Cretaceous plesiosaurs. *University of California publications in the Geological sciences* **44**, 1-96 (1962).
86 Galton, P. M. & Upchurch, P. in *The Dinosauria* (eds D B Weishampel, P Dodson, & H Osmólska) 343-362 (University of California Press, 2004).
87 Currie, P. J., Badamgarav, D., Koppelhus, E. B., Sissons, R. & Vickaryous, M. K. Hands, feet, and behaviour in Pinacosaurus (Dinosauria: Ankylosauridae). *Acta Palaeontol Pol* **56**, 489-504 (2011).
88 Gilmore, C. W. On dinosaurian reptiles from the Two Medicine Formation of Montana. Proceedings of the United States National Museum, 77, 1-39 (1930).
89 Gilmore, C. W. & Granger, W. Two new dinosaurian reptiles from Mongolia: with notes on some fragmentary specimens. American Museum novitates; no. 679. (1933).
90 Burns, M. *Intraspecific Variation in Late Cretaceous Nodosaurids (Ankylosauria: Dinosauria)* Ph.D thesis, University of Alberta, (2015).

91 Ősi, A., Prondvai, E., Mallon, J. & Bodor, E. R. Diversity and convergences in the evolution of feeding adaptations in ankylosaurs (Dinosauria: Ornithischia). *Hist Biol* **29**, 539-570 (2017).
92 Arbour, V. M., Burns, M. E., Bell, P. R. & Currie, P. J. Epidermal and dermal integumentary structures of ankylosaurian dinosaurs. *J Morphol* **275**, 39-50 (2014).
93 Norman, D. B. *Scelidosaurus harrisonii* from the Early Jurassic of Dorset, England: cranial anatomy. *Zool J Linn Soc* **188**, 1-81, doi:10.1093/zoolinnean/zlz074 (2019).
94 Sereno, P. C. *Lesothosaurus*, "fabrosaurids", and the early evolution of Ornithischia. *J Vertebr Paleontol* **11**, 168-197 (1991).
95 Sereno, P. C. & Dong, Z. The skull of the basal stegosaur *Huayangosaurus taibaii* and a cladistic diagnosis of Stegosauria. *J Vertebr Paleontol* **12**, 318-343 (1992).
96 Colbert, E. H. *A Primitive Ornithischian Dinosaur from the Kayenta Formation of Arizona*. 55 (Museum of Northern Arizona Press, 1981).
97 Galton, P. M. Skull bones and endocranial casts of stegosaurian dinosaur *Kentrosaurus* Hennig, 1915 from Upper Jurassic of Tanzania, East Africa. *Geol Palaeontol* **22**, 123-143 (1988).
98 Carpenter, K., Miles, C. A. & Cloward, K. New primitive stegosaur from the Morrison Formation, Wyoming. *The armored dinosaurs*, 55-75 (2001).
99 Kinneer, B., Carpenter, K. & Shaw, A. Redescription of *Gastonia burgei* (Dinosauria: Ankylosauria, Polacanthidae), and description of a new species. *Neues Jahrbuch für Geologie und Paläontologie-Abhandlungen* **282**, 37-80 (2016).
100 Coombs, W. & Maryanska, T. in *The Dinosauria* (eds Weishampel DB, Dodson P, & Osmolka H) 456–483 (University of California Press, 1990).
101 Galton, P. M. & Carpenter, K. The plated dinosaur *Stegosaurus longispinus* Gilmore, 1914 (Dinosauria: Ornithischia; Upper Jurassic, western USA), type species of *Alcovasaurus* n. gen. *Neues Jahrbuch für Geologie und Paläontologie, Abhandlungen* **279**, 185-208 (2016).
102 Ostrom, J. H. *Stratigraphy and paleontology of the Cloverly Formation (Lower Cretaceous) of the Bighorn basin area, Wyoming and Montana*. (Yale University Press, 1970).
103 Carpenter, K. Skeletal reconstruction and life restoration of *Sauropelta* (Ankylosauria: Nodosauridae) from the Cretaceous of North America. *Can J Earth Sci* **21**, 1491-1498 (1984).
104 Arbour, V. M. & Evans, D. C. A new ankylosaurine dinosaur from the Judith River Formation of Montana, USA, based on an exceptional skeleton with soft tissue preservation. *Royal Society Open Science* **4**, 161086 (2017).
105 Zheng, W. *et al.* The most basal ankylosaurine dinosaur from the Albian–Cenomanian of China, with implications for the evolution of the tail club. *Scientific reports* **8**, 1-17 (2018).

106 Brown, C. M. *et al.* An exceptionally preserved three-dimensional armored dinosaur reveals insights into coloration and Cretaceous predator-prey dynamics. *Curr Biol* **27**, 2514-2521. e2513 (2017).
107 Parks, J.-Y. *et al.* Additional skulls of *Talarurus plicatospineus* (Dinosauria: Ankylosauridae) and implications for paleobiogeography and paleoecology of armored dinosaurs. *Cretaceous Res* **108**, 104340 (2020).
108 Coria, R. A. & Salgado, L. in *The armored dinosaurs* (ed Carpenter. K.) 159-168 (Indiana University Press, 2001).
109 Raven, T. J., Barrett, P. M., Pond, S. B. & Maidment, S. C. Osteology and Taxonomy of British Wealden Supergroup (Berriasian–Aptian) Ankylosaurs (Ornithischia, Ankylosauria). *J Vertebr Paleontol* **40**, e1826956 (2020).
110 Maleev, E. The armored dinosaurs of the Cretaceous Period in Mongolia (family Syrmosauridae). *Trudy Paleontologičeskaâ Institut, Akademiâ Nauk SSSR* **48**, 142-170 (1954).
111 Penkalski, P. & Tumanova, T. The cranial morphology and taxonomic status of Tarchia (Dinosauria: Ankylosauridae) from the Upper Cretaceous of Mongolia. *Cretaceous Res* **70**, 117-127 (2017).
112 Penkalski, P. Revised systematics of the armoured dinosaur *Euoplocephalus* and its allies. *Neues Jahrbuch für Geologie und Paläontologie-Abhandlungen*, 261-306 (2018).
113 Carpenter, K., Bartlett, J., Bird, J. & Barrick, R. Ankylosaurs from the Price River Quarries, Cedar Mountain Formation (Lower Cretaceous), east-central Utah. *J Vertebr Paleontol* **28**, 1089-1101 (2008).
114 Lü, J., Ji., Q., Gao, J.. & Li., Z. A new species of the ankylosaurid dinosaur *Crichtonsaurus* (Ankylosauridae: Ankylosauria) from the Cretaceous of Liaoning Province, China. *Acta Geologica Sinica-English Edition* **81**, 883-897 (2007).
115 Godefroit, P., Pereda-Suberbiola, X., Li, H. & Dong, Z.-M. A new species of the ankylosaurid dinosaur *Pinacosaurus* from the Late Cretaceous of Inner Mongolia (PR China). *Bulletin de l'Institut Royal des Sciences Naturelles de Belgique, Sciences de la terre* **69**, 17-36 (1999).
116 Pang, Q. & Cheng, Z. A new ankylosaur of Late Cretaceous from Tianzhen, Shanxi. *Progr Nat Sci* **8**, 326-334 (1998).
117 Penkalski, P. & Blows, W. T. *Scolosaurus cutleri* (Ornithischia: Ankylosauria) from the Upper Cretaceous Dinosaur Park Formation of Alberta, Canada. *Can J Earth Sci* **50**, 171-182 (2013).
118 Arbour, V. M. & Currie, P. J. *Euoplocephalus tutus* and the diversity of ankylosaurid dinosaurs in the Late Cretaceous of Alberta, Canada, and Montana, USA. *PLoS ONE* **8**, e62421 (2013).
119 Parks, W. *Dyoplosaurus acutosquameus*, new genus and species of armoured dinosaurs; and notes on a skeleton of *Prosaurolophus maximus*. *University of Toronto Studies Geological Series.* **8**, 1-35 (1924).
120 Arbour, V. M., Burns, M. E. & Sissons, R. L. A redescription of the ankylosaurid dinosaur *Dyoplosaurus acutosquameus* Parks, 1924 (Ornithischia:

Ankylosauria) and a revision of the genus. *J Vertebr Paleontol* **29**, 1117-1135 (2009).

121 Maidment, S. C., Wei, G. & Norman, D. B. Re-description of the postcranial skeleton of the Middle Jurassic stegosaur *Huayangosaurus taibaii*. *J Vertebr Paleontol* **26**, 944-956 (2006).

122 Mallison, H. The real lectotype of *Kentrosaurus aethiopicus* HENNIG, 1915. *Neues Jahrbuch für Geologie und Paläontologie-Abhandlungen*, 197-206 (2011).

123 Gilmore, C.W. Osteology of the armoured Dinosauria in the United States National Museum, with special reference to the genus Stegosaurus. United States National Museum Bulletin 89, 1–143 (1914).

124 Maidment, S. C. R., Brassey, C. & Barrett, P. M. The postcranial skeleton of an exceptionally complete individual of the plated dinosaur *Stegosaurus stenops* (Dinosauria: Thyreophora) from the Upper Jurassic Morrison Formation of Wyoming, USA. *PLoS ONE* **10**, e0138352 (2015).